A NUMERICAL AND EXPERIMENTAL STUDY OF TURBULENT BOUNDARY LAYER WITH ROD-ROUGHENED WALL

Seung-Hyun Lee
Department of Mechanical Engineering,
Korea Advanced Institute of Science and Technology,
373-1, Guseong-dong, Yusong-gu, Daejeon, 305-701, South Korea,
leehuiso@kaist.ac.kr

Hyung Jin Sung
Department of Mechanical Engineering,
Korea Advanced Institute of Science and Technology,
373-1, Guseong-dong, Yusong-gu, Daejeon, 305-701, South Korea,
hjsung@kaist.ac.kr

ABSTRACT

The effects of surface roughness on a turbulent boundary layer (TBL) were investigated using direct numerical simulations (DNS) and particle image velocimetry (PIV). The roughness elements used were periodically arranged two-dimensional spanwise rods, and the roughness height was k/δ=0.05 for DNS and k/δ=0.0165, 0.032 for PIV. In PIV measurements, the friction velocity u_τ for smooth and rough walls was estimated by fitting of mean velocity profile. Introduction of the roughness elements increased the wake strength and the turbulent stress not only in the roughness sublayer but also in the outer layer. This indicates the existence of interaction between inner and outer layers. Iso-contours of mean velocities and Reynolds stresses in the roughness sublayer obtained by PIV measurements show a good agreement with DNS results.

INTRODUCTION

Turbulent boundary layers (TBLs) are observed in numerous fluid dynamic engineering applications, and many experimental and numerical studies have examined the characteristics of TBLs. In real engineering applications involving wall-bounded boundary layer flow (e.g. automobiles, ships, airplanes, heat-exchangers, and weather prediction), the roughness of the wall surface is an important design parameter because it influences characteristics such as the transport of heat, mass and momentum. Although the effects of surface roughness on a TBL have been examined in many experimental and numerical studies, knowledge of these effects remains incomplete.

Previous studies on the effect of surface roughness on a TBL are well reviewed by Raupach et al. (1991) and Jimenez (2004). These reviews support the wall similarity hypothesis of Townsend (1976), which states that outside the roughness sublayer turbulent motions are independent of the surface roughness and that the interaction between the inner and outer layers is very weak at sufficiently large Reynolds numbers. In further support of this similarity hypothesis, Schultz and Flack (2005), Flack et al. (2005) and Connelly et al. (2006) recently observed that the outer layers of flows past smooth and rough walls were similar in terms of both mean flow and turbulent statistics.

However, results from several experimental studies have been contrary to the wall similarity hypothesis. Krogstad et al. (1992) showed that the wake strength in a TBL is increased by surface roughness and that the interaction between the inner and outer layers is non-negligible. Krogstad and Antonia (1999) and Keirsbulck et al. (2002) observed that turbulent Reynolds stresses in the outer layer of a TBL are significantly affected by the surface roughness. Smalley et al. (2002) found that a TBL against a rough wall exhibits lower anisotropy than that against a smooth wall. Bandyopadhyay and Watson (1988) and Antonia and Krogstad (2001) also observed that variations in the surface roughness significantly affect the high-order statistics in the outer layer. These experimental results oppose the notion that the outer layer of a TBL is insensitive to the surface roughness, and have led to considerable uncertainty regarding the effects of surface roughness on TBLs.

Recently, several numerical studies using direct numerical simulation (DNS) and large eddy simulation (LES) have been conducted on turbulent channel flow with a rough wall (e.g. Asrafian et al. 2004; Bhaganagar et al. 2004; Lee 2002; Leonardi et al. 2003). Krogstad et al. (2005) compared the experimental and numerical results for turbulent flow in a symmetric channel with a rod-roughness and showed no significant difference between the characteristics of the outer layer of rough and smooth walls. They conjectured that the degree to which surface roughness affects the outer layer is influenced by the flow type, for example symmetric channel flow, asymmetric channel flow, boundary layer, and so on.

Despite the fact that most experimental studies have examined the characteristics of TBLs, the majority of numerical studies (LES and DNS) have examined turbulent channel flows. This discrepancy can be attributed to the difficulty of simulating TBLs and the absence of DNS data

for these systems has made it difficult to validate experiments on rough-wall TBLs.

Recently, Lee and Sung (2007) carried out the first DNS of TBLs with rough and smooth walls and examined the spatially-developing characteristics of the rough-wall TBL. They suggestedd that introduction of the roughness elements affects the turbulent stresses and vertical turbulent transport not only in the roughness sublayer but also in the outer layer. Those lack of surface similarity between rough and smooth walls indicates the strong interaction between the inner and outer layers induced by the surface roughness and it is contrary to the previous findings of a DNS study of turbulent channel flow with the same 2-D rod-roughened wall. They proposed that the wall similarity criteria may be not universal to all flow types and supported the conjecture that the surface roughness effects on the outer layer depends on the outer boundary condition.

In the present study, we carried out PIV measurements on TBLs with rough and smooth walls and compared experimatal results with numerical results to validate our findings of DNS (Lee and Sung 2007). The objective of the present study was to elucidate the interaction between the inner and outer layers arising from the roughness and to delineate the basic characteristics of a rough-wall TBL.

NUMERICAL AND EXPERIMENTAL DETAILS

Numerical details

Direct numerical simulations of TBLs with smooth and rough walls were performed. A schematic diagram of the TBL with rough wall, and the roughness shape is shown in figure 1. The domain size was $768\theta_{in}\times60\theta_{in}\times80\theta_{in}$ for rough wall and $1536\theta_{in}\times60\theta_{in}\times80\theta_{in}$ for smooth wall in the streamwise, wall-normal and spanwise directions, where the corresponding mesh number is 2049×150×257 for rough and smooth walls. The domain size in the streamwise direction was sufficiently long that the effects of the surface roughness step change could be neglected. Realistic velocity fluctuations at the inlet were provided based on the method of Lund, Wu & Squires (1998). Before the main simulation, an auxiliary simulation was carried out to obtain the inflow data. The Reynolds number at the inlet for both cases was $Re_{\theta,in}$=300. The convective outflow condition was used at the exit and the no-slip boundary condition was imposed at the solid wall. At the free-stream, the conditions $u=U_\infty$ and $\partial v/\partial y=\partial w/\partial y=0$ were imposed. Periodic boundary conditions were used in the spanwise direction. The governing equations for an incompressible Newtonian fluid, the Navier-Stokes equation and the continuity equation are integrated in time using the fully implicit fractional step method proposed by Kim et al. (2002). All terms are advanced with the Crank-Nicholson method in time, and they are resolved with the second-order central difference scheme in space. Based on a block LU decomposition, both velocity-pressure decoupling and additional decoupling of the intermediate velocity components are achieved with the approximate factorization. The immersed boundary method is used to efficiently describe the rough surface with Cartesian coordinates and a rectangular domain (Kim et al. 2001). The discrete-time momentum forcing is calculated explicitly in time to satisfy the no-slip condition on the immersed boundary using the previous velocity field near the forcing point. Direct numerical simulations of the TBL over a rough or smooth wall were performed by means of a parallel computation using 32 CPUs of a supercomputer (IBM p690+). More detailed description of numerical simulation is described in Lee and Sung (2007).

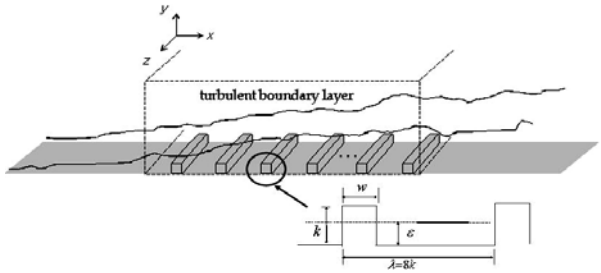

Figure 1 Schematic diagrams of computational domain and rod roughness.

Experimental details

Measurements were performed in a recirculating open-water channel driven by a centrifugal pump. A setting chamber, a honeycomb, and a contraction were placed in sequence to ensure flow homogeneity. Figure 2 shows a schematic diagram of the test section, roughness elements and PIV experimental setup. The dimensions of the test section were 250mm (width) × 275mm (depth) × 2000mm (length). The boundary layer was tripped at the leading edge of the flat plate using a combination of a trip wire of diameter 3mm and a sand grain (CC-80Cw) rough strip. This combination ensured a self-preserving turbulent boundary layer upstream of the first rod roughness.

CCD camera (Kodak ES-1.0, 1024×1024 pixel CCD array size) coupled to a PC running image acquisition software was used to acquire images. The flow plane of interest was illuminated with a two head Nd:YAG laser (Big Sky Laser, Ultra). The pulses for the laser and the CCD camera were generated and delayed using a pulse generator (Berkeley Nucleonics, BNC-555). The iterative multigrid image processing method (Scarano and Riethmuller 1999) was used to increase the spatial resolution and CBC (Correlation based Correction, Hart 1999) was used to improve the signal-to-noise ratio. For vector post-processing, the local median filter criterion (Westerweel 1994) was used. The field of view of camera was about 100mm×100mm for smooth and rough walls. At each measurement, 1600 velocity fields were acquired. The final interrogation window size was 32×32 pixels with a 50% overlap. This gave a spatial resolution of 1.6mm between measurement points. This corresponds to about 1~2 vectors across the face of the roughness elements and the spatial resolution is very coarse to accurately represent turbulence statistics in the roughness sublayer. Therefore high-resolution PIV measurement was also carried out. In this case, the field of view of camera was about 26.3mm×26.3mm and 4800 velocity fields were acquired. This gave a spatial resolution of 0.42mm between measurement points, which corresponds to 6 vectors across the face of the roughness element.

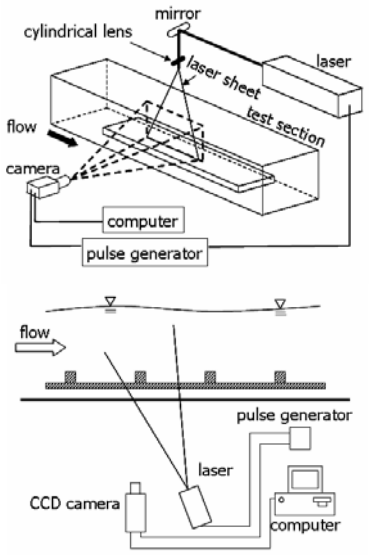

Figure 2 Schematic diagrams of schematic diagram of the test section, roughness elements and PIV experimental setup.

Roughness elements

The roughness takes the form of two-dimensional spanwise rods with a square cross-section that are periodically arranged in the streamwise direction with a pitch of $\lambda=8k$. In DNS, the roughness height is $k=1.5\theta_{in}$, which corresponds to $k/\delta=0.045\sim0.125$ and $k^+=32\sim45$. The first rod is placed at $80\theta_{in}$ downstream from the inlet, the surface condition therefore changes abruptly from smooth to rough at this location, which is defined as $x=0$. After the roughness step change, there is a transient region in which the flow adapts to the new boundary conditions and the domain size along the streamwise direction should be large to reach a new equilibrium state where a self-preservation form is achieved.

As shown in figure 3, rough-wall turbulent boundary layer in DNS reached the equilibrium state. Self-preservation forms of Reynolds stresses are obtained in the outer layer after $x=324\theta_{in}$. In this region, the friction velocity and shape parameter (H) converges to a constant value. In DNS, all the data for the rough wall turbulent boundary layer were obtained at a location sufficiently downstream ($x=516\theta_{in}$) that the flow had achieved the equilibrium state. The smooth wall data were obtained at $x=1098\theta_{in}$, where the boundary layer thickness is the same as that of the rough wall. In PIV measurements, the height of each rod is 1.1mm and 2.0mm. The rods are placed from 700mm to 1300mm downstream from the leading edge of the plate. In PIV measurements, figure 4 shows that the Reynolds stresses of rough walls normalized by free stream velocity increase only in $y/\delta<0.6$. This indicates that the Reynolds stresses increased near the roughness are not propagated to the whole boundary layer and rough-wall turbulent boundary layers in experiments are not reached to an equilibrium state at the end of the test section. All the data for the PIV measurements were obtained near the end of the test section. Table 1 summarized smooth and rough cases examined by DNS and PIV and various roughness parameters.

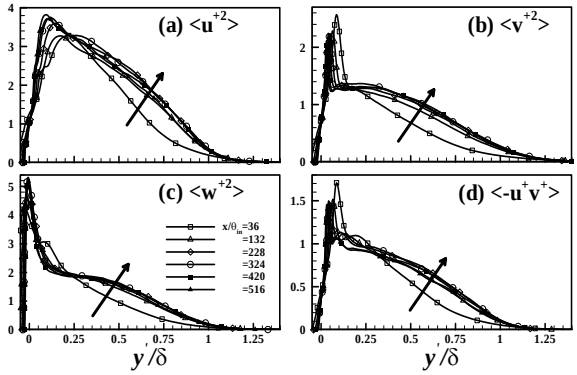

Figure 3 Variations of turbulent Reynolds stresses (R1) along the downstream, normalized by u_τ^2.

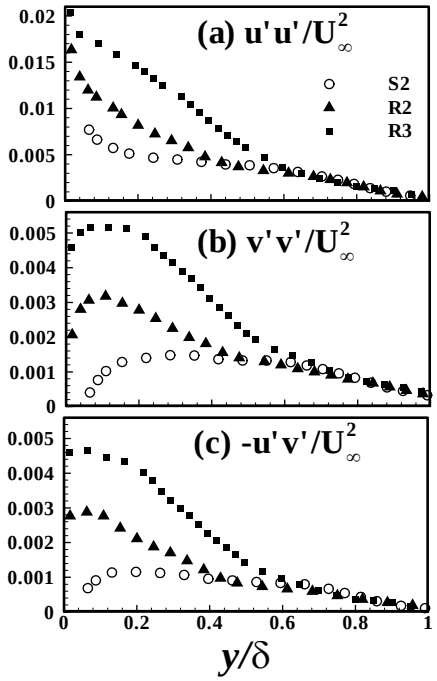

Figure 4 Reynolds stresses near the end of the test section, normalized by U_∞^2

Table 1: Cases examined and roughness parameters..

Case	Reθ	k/δ	k^+	k_s^+	ΔU^+
S1 (DNS)	1098	-	-	-	-
R1 (DNS)	1351	0.050	33.1	211.5	9.7
S2 (PIV)	1232	-	-	-	-
R2 (PIV)	1216	0.0165	11.8	13.2	3.1
R3 (PIV)	1550	0.0320	26.0	87.3	7.7

Friction velocity

In DNSs, skin frictional drag and form drag can be directly calculated from wall shear stress and wall pressure data. The friction velocity u_τ was estimated from the total drag, which is a sum of the skin frictional and form drags. The skin frictional drag and form drag are spatially-

averaged over one pitch λ, that is, the distance between adjacent rods.

In PIV measurements, the friction velocity u_τ for smooth and rough walls can be estimated by fitting of mean velocity profile (Krogstad et al. 1992). For smooth walls, u_τ by CPM method is also compared. The friction velocity of smooth wall using the two methods agreed to within about 3%. For rough walls, the other estimate for friction velocity was obtained by extrapolating the measured turbulent shear stress to the wall. The friction velocity of two rough walls using the two methods agreed well within about 7%. In the present study, we used the friction velocity estimated by the fitting method.

RESULTS

Mean velocity

The mean streamwise velocity profiles for smooth and rough walls are shown in figure 5. The general mean velocity shift (ΔU^+) is clearly shown for rough wall TBLs. For smooth TBL, the wake strength of S2 is much smaller than that of S1. Decrease of wake strength may be due to the existence of free stream tubulence near the free surface of open water channel. For rough wall cases (R2 and R3), wake strength is larger than smooth wall, indicating that surface roughness increases wake strength. This is consistent with the experiment of Krogstad et al. (1992). The velocity defect profiles of the smooth and rough walls are displayed in Figure 5 (b). There is difference between DNS and PIV results due to the different wake strength. However, each DNS and PIV result shows a good surface similarity in the outer layer.

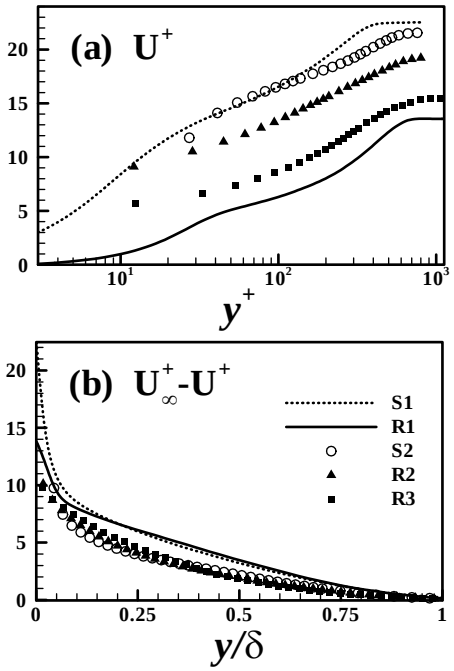

Figure 5 Mean velocity profiles.

Reynolds stresses

The Reynolds stresses are compared in Figure 6 for the smooth and rough walls. In DNS, the wall-normal stresses $<v^{+2}>$ and Reynolds shear stresses $<-u^+v^+>$ of rough TBL exhibit increase in the whole boundary layer. In PIV measurements, Reynolds stresses of rough TBL increase in $y/\delta<0.4$ and decreased in $y/\delta>0.4$. The decrease in $y/\delta>0.4$ may be due to the lack of self-preservation for rough TBLs. The depth of roughness sublayer as 5 times of roughness height, the $5k/\delta$ for each rough wall TBLs is 0.25 (R1), 0.0823 (R2) and 0.160 (R3). This indicates that the roughness effects on Reynolds stresses are propagated beyond roughness sublayer and Reynolds stress profiles normalized by the friction velocity do not show a good surface similarity between the rough and smooth wall cases.

Jimenez (2004) suggested a criterion for surface similarity that δ/k has to be larger than 40 before wall similarity can be expected. Schultz & Flack (2005) proposed that the extent of the roughness sublayer is $5k_s$ rather than $5k$ and the turbulence structure will not be changed when the extent of the roughness sublayer is smaller than the inner layer itself ($5k_s<0.2\delta$). In the present rough TBLs, R3 case, the smallest rod roughness, satisfies both of cirteria, however, it also shows lack of surface similarity in outer layer. This indicates that the above criteria should be further investigated whether it can be applied to all flow types or roughness types generally.

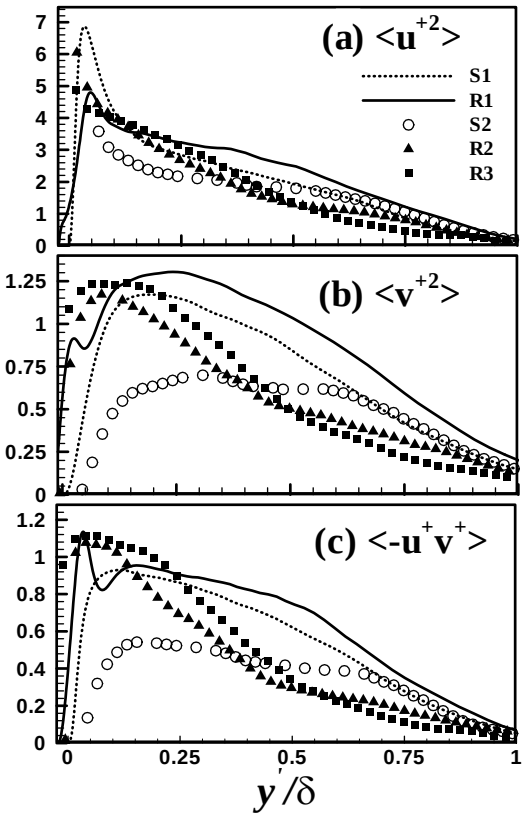

Figure 6 Reynolds stresses in the outer coordinateds, normalized by u_τ^2

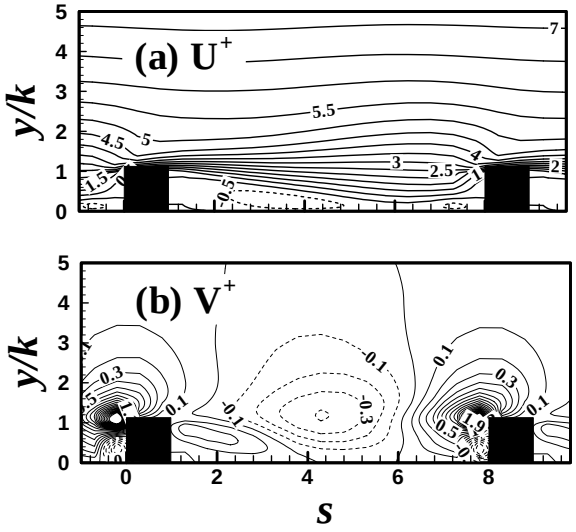

Figure 7 Iso-contours of mean velocities in the roughness sublayer (DNS).

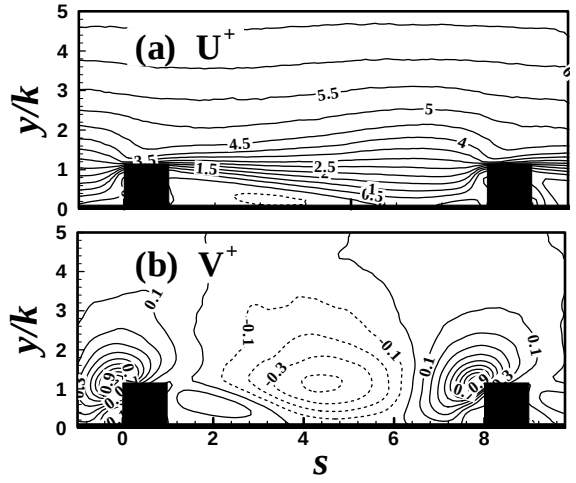

Figure 8 Iso-contours of mean velocities in the roughness sublayer (PIV).

Roughness sublayer

Introduction of the rod roughness elements onto the smooth surface significantly affects the turbulent flow structures, leading to very high turbulent intensities in the vicinity of the wall. This near-wall region, which is known as the roughness sublayer, is generally assumed to have a height of 2~5 times the roughness height. Lee and Sung (2007) studied the characteristics of roughness sublayer (y<5k) using DNS. One of the benefits of PIV compared to other measurment techniques is its ability to measure 2D velocity field. In the present study, we obtained the turbulence statistics in the roughness sublayer (R3) using PIV measurements and compared with DNS results (R1).

Figure 7 and 8 show iso-contours of mean velocities in the roughness sublayer obtained by DNS and PIV. They show an excellent agreement between DNS and PIV. Figure 9 and 10 show iso-contours of Reynolds stresses in the roughness

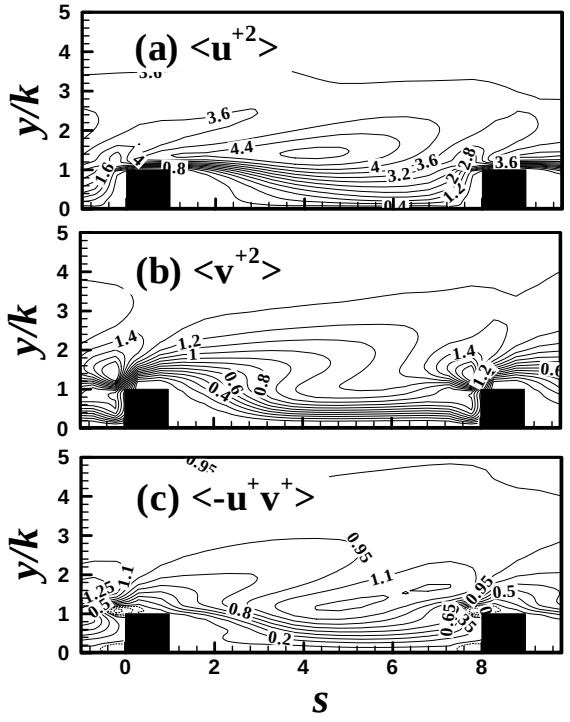

Figure 9 Iso-contours of Reynolds stresses in the roughness sublayer (DNS).

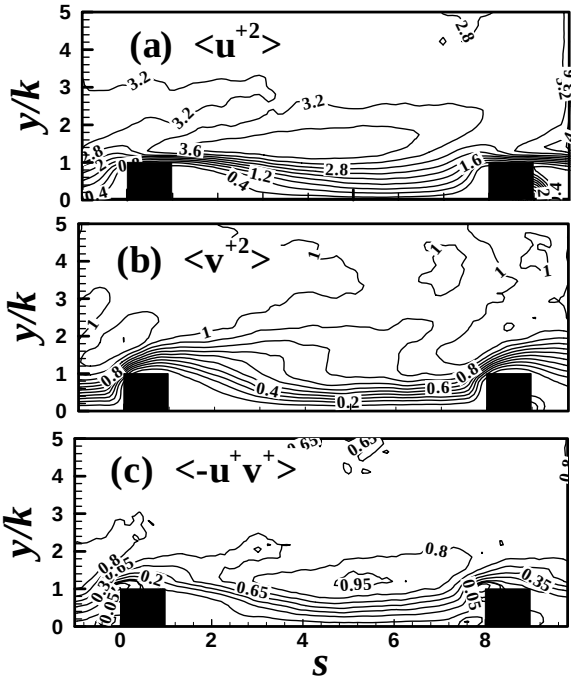

Figure 10 Iso-contours of Reynolds stresses in the roughness sublayer (PIV).

sublayer obtianed by DNS and PIV. They show a good agreement between DNS and PIV. This suggests that PIV is very good measurement techniques to investigate the effect of roughness in the roughness sublayer.

CONCLUSION

A numerical and experimental study was carried out to investigate the effects of surface roughness on a turbulent boundary layer using DNS and PIV. The roughness elements used were periodically arranged two-dimensional spanwise rods, and the roughness height was k/δ=0.05 for DNS and k/δ=0.0165, 0.032 for PIV. In PIV measurements, the friction velocity u_τ for smooth and rough walls was estimated by fitting of mean velocity profile. Results show that introduction of the roughness elements increased the wake strength and the turbulent stress not only in the roughness sublayer but also in the outer layer. This indicates the existence of interaction between inner and outer layers. Iso-contours of mean velocities and Reynolds stresses in the roughness sublayer obtained by PIV measurements show a good agreement with DNS results.

ACKNOWLEDGEMENTS

This work was supported by the Basic Research Program (R01-2004-000-10521-0) of the Korea Science & Engineering Foundation and partially supported by the Grand Challenge Supercomputing Program of the Korea Institute of Science and Technology Information with Drs Lee and Ali as the technical support.

REFERENCES

Antonia, R. A. and Krogstad, P. –Å., 2001, "Turbulent Structure in Boundary Layers over Different Types of Surface Roughness", Fluid Dyn. Res. Vol. 28, pp. 139-157.

Ashrafian, A. and Andersson, H. I., 2006, "The Structure of Turbulence in a Rod-roughened Channel", Int. J. Heat and Fluid Flow, Vol. 27, pp. 65-79.

Ashrafian, A., Andersson, H. I. and Manhart, M., 2004, "DNS of Turbulent Flow in a Rod-roughened Channel", Int. J. Heat and Fluid Flow, Vol. 25, pp. 373-383.

Bandyopadhyay, P. R. and Watson, R. D., 1988, "Structure of Rough-wall Boundary Layers", Phys. Fluids, Vol. 31, pp. 1877-1883.

Bhaganagar, K., Kim, J. and Coleman, G., 2004, "Effect of Roughness on Wall-bounded Turbulence", Flow, Turbulence and Combustion, Vol. 72, pp. 463-492.

Connelly, J. S., Schultz, M. P. and Flack, K. A., 2006, "Velocity-defect Scaling for Turbulent Boundary Layers with a Range of Relative Roughness", Exp. Fluids, Vol. 40, pp. 188-195.

Flack, K. A., Schultz, M. P. and Shapiro, T. A., 2005, "Experimental Support for Townsend's Reynolds Number Similarity", Phys. Fluids, Vol. 17, 035102.

Hart, D. P., 2000, "PIV Error Correction", Exp. Fluids, Vol. 29, pp. 13-22.

Jimenez, J., 2004, "Turbulent Flows over Rough Walls", Annu. Rev. Fluid Mech., Vol. 36, pp. 173-196.

Keirsbulck, L., Labraga, L., Mazouz, A. and Tournier, C., 2002, "Surface Roughness Effects on Turbulent Boundary Layer Structures", J. Fluids Engineering, Vol. 124, pp. 127-135.

Kim, J., Kim, D. and Choi, H., 2001, "An Immersed Boundary Finite-volume Method for Simulations of Flow in Complex Geometries", J. Computaionl Physics, Vol. 171, pp. 132-150.

Kim, K., Baek, S.-j. and Sung, H. J., 2002, "An Implicit Velocity Decoupling Procedure for the Incompressible Navier-Stokes Equations", Int. J. Numer. Meth. Fluids, Vol. 38, pp. 125-138.

Krogstad, P. -Å., Antonia, R. A. and Browne, L. W. B., 1992, "Comparison between Rough- and Smooth-wall Turbulent Boundary Layers", J. Fluid Mechanics, Vol. 245, pp. 599-617.

Krogstad, P. -Å. and Antonia, R. A., 1999, "Surface Roughness Effects in Turbulent Boundary Layers", Exp. Fluids, Vol. 27, pp. 450~460.

Krogstad, P. –Å., Andersson, H. I., Bakken, O. M. and Ashrafian, A., 2005, "An Experimental and Numerical Study of Channel flow with Rough Walls", J. Fluid Mechanics, Vol. 530, pp. 327-352.

Lee, C., 2002, "Large-eddy Simulation of Rough-wall Turbulent Boundary Layers", AIAA J., Vol. 40, pp. 2127-2130.

Lee, S. -H. and Sung, H. J., 2007, "Direct Numerical Simulation of the Turbulent Boundary Layer over a Rod-roughened Wall", J. Fluid Mechanics, in press.

Leonardi, S., Orlandi, P., Smalley, R.J., Djenidi, L. and Antonia, R.A., 2003, "Direct Numerical Simulations of Turbulent Channel Flow with Transverse Square Bars on One Wall", J. Fluid Mechanics, Vol. 491, pp. 229-238.

Lund, T. S., Wu, X. and Squires, K. D., 1998, "Generation of Turbulent Inflow Data for Spatially-Developing Boundary Layer Simulation", J. Comput. Phys., Vol. 140, pp. 233-258.

Raupach, M. R., Antonia, R. A. and Rajagopalan, S., 1991, "Rough-wall Turbulent Boundary Layers", Appl. Mech. Rev., Vol. 44, pp. 1-25.

Scarno, F. and Riethmuller, M. L., 1999, "Iterative Multigrid Approach in PIV Image Processing with Discrete Window Offset", Exp. Fluids, Vol. 26, pp. 513-523.

Schultz, M. P. and Flack, F. A., 2005, "Outer Layer Similarity in Fully Rough Turbulent Boundary Layers", Exp. Fluids, Vol. 38, pp. 328-340.

Smalley, R. J., Leonardi, S., Antonia, R. A., Djenidi, L. and Orlandi, P., 2002, "Reynolds Stress Anisotropy of Turbulent Rough Wall Layers", Exp. Fluids, Vol. 33, pp. 32-37.

Townsend, A. A., 1976, "The Structure of Turbulent Shear Flow," Cambridge University Press, Cambridge.

Westerweel, J., 1994, "Efficient Detection of Spurious Vectors in Particle Image Velocimetry Data", Exp. Fluids, Vol. 16, pp. 236-247.